UDC 621.3 DOI: 10.46972/2076-1546.2025.28.05

V. V. Pozdniakov

CFAR ALGORITHM APPLICATION FOR DETECTING ACOUSTIC SIGNALS HARMONIC COMPONENTS OF PROPELLER AERIAL ATTACK WEAPON

The article is devoted to the detection of harmonic components in the acoustic signal spectrum of propeller aerial attack weapon. The received acoustic signal may contain harmonics of both one and several radiation sources. By analyzing the frequency values of the harmonic components with regard to the Doppler shift and their distribution along the frequency axis, it is possible to determine the number of radiation sources and estimate their motion parameters. Detecting harmonic components in the background noise is difficult because its spectral density is uneven and unknown. To solve this problem, it is proposed to use an adaptive thresholding method, an algorithm with a constant false alarm rate, which is used to detect radar signals, as it is able to track changes in noise levels. The spectrum of the acoustic signal is analyzed and the numerical values of the parameters necessary for tuning the algorithm are determined. A comparison was made between three different approaches to assessing background noise levels and calculating detection thresholds, including cell averaging-, smallest-of cell averaging-, and order statistics-constant false alarm rate. The parameters of the algorithm have been determined, which allow us to build a threshold that provides tracking of noise level changes and detection of both strong and weak harmonics in the spectrum of an acoustic signal.

The experimental results show that the proposed method allows detecting 45% more harmonics compared to the consecutive mean excision algorithm and 26% more harmonics compared to the moving average algorithm. The results obtained can be used to improve existing and develop new devices and systems for acoustic monitoring of airspace.

Keywords: *aerial attack weapon; acoustic signal; CFAR algorithm; frequency spectrum; harmonic component; threshold.*

Problem statement in general. To strike energy and infrastructure facilities deep inside the country, the enemy widely uses propeller-driven aerir attack weapons (AAW) together with air-, sea-, and ground-based missile weapons. In addition, they can perform reconnaissance, surveillance, diversion, and air defense system exhaustion functions. Their relatively low speed and flight altitude make it possible to detect such AAW using acoustic means.

The acoustic signal of a screw motor AAW is polyharmonic with continuous noise components in frequency [1]. The noise level is uneven, so using a fixed threshold to separate signal and noise counts in the frequency domain will result in the omission of weak high-frequency harmonic components, which will impair subsequent stages of signal processing, in particular the search for multiple harmonics.

CFAR (constant false alarm rate) algorithms are used to detect short-term signals against a background of noise with unknown and uneven density [2]. Currently, there are many known

modifications of such algorithms, but for each specific case (type of signal-to-noise environment), it is necessary to select the type of algorithm and determine its parameters.

Analysis of the latest research and publications. Recently, scientists in many countries have been actively using CFAR algorithms in both theoretical and applied research, constantly modifying, improving, and applying them in various fields of signal processing.

In [3], a modern deep neural network was modified using the CFAR algorithm to solve the problem of detecting multi-scale vessels on radar images. Using object proposals generated by the network for the guard intervals of the CFAR algorithm, this method detects small targets. In [4], a method for regulating the pruning of a deep neural network based on the CFAR algorithm is proposed. It allows for the adaptive removal of some neural nodes and the optimization of neural nodes involved in the calculation. This helps to reduce the amount of memory used and prevents excessive parameterization.

Publication [5] discusses the detection of multiple objects on an acoustic image from a multibeam sonar. The proposed method is effective and robust in a multi-object environment, especially when the objects are close to each other.

Papers [6–8] are devoted to the development of methods and approaches based on the use of CFAR detectors for detecting network intrusions and security threats in computer networks.

In [9], a comprehensive method for localizing cable defects based on frequency reflectometry and the CFAR algorithm is proposed. The localization spectrum data is substituted into CFAR to obtain a threshold and extract information about the effective amplitude of the cable and the corresponding position of the defect.

[10] describes an algorithm for detecting leaks in pipelines based on acoustic sensor signals using a CFAR detector. A field experiment was conducted and confirmed the possibility of using this type of algorithm to detect leaks in real time.

However, among all the works, there are no studies on the adaptation of CFAR algorithms for detecting harmonic components of acoustic signals of AAW.

Formulation of the research task. The aim of the study is to increase the number of detected harmonic components of the acoustic signal of the AAW by selecting and adapting the parameters of the CFAR algorithm. To do this, it is necessary to analyze known CFAR algorithms, the conditions for their application, and select the necessary algorithm and its parameters, taking into account the characteristics of the frequency spectrum of acoustic signals from screw-motor AAW.

Core material

Structure of the acoustic signal of a screw motor AAW in the frequency domain

The acoustic signal of screw-driven AAW equipped with a piston engine with an air screw is quite complex. It includes a series of harmonic and continuous noise-like components [1]. The frequency of harmonic components is an informational parameter of the signal. It can be used to detect AAW and determine their number in groups. The received acoustic signal may contain harmonics from one or several radiation sources. By analyzing the frequencies of harmonic components, taking into account the Doppler shift and their distribution along the frequency axis, it is possible to determine the number of radiation sources and estimate the parameters of their movement.

Periodogram methods for obtaining spectral estimates, based on data conversion using fast Fourier transform (FFT) and subsequent averaging, are the most robust spectral estimation methods and can therefore be applied to almost all classes of signals and noise with stationary properties. In addition, spectral estimation methods based on FFT calculations are the most appropriate in terms of computational complexity [11]. Therefore, we will use periodogram estimates to calculate the energy spectrum of an acoustic signal. Let us consider the case without averaging spectral estimates.

The spectral power density (SPD) of the signal is calculated using Welch's periodogram. First, we determine the sample spectrum of the weighted window of the j-th segment of the signal using the following expression:

$$X_j(k) = \sum_{n=0}^{N_{FFT}-1} x(n)w(n)e^{-j2\pi\frac{kn}{N_{FFT}}}, \quad (1)$$

where $x(n)$ – n-th received signal count;

N_{FFT} – length of the FFT;

$w(n)$ – n-th window function count.

We can take adjacent signal fragments with overlap. R counts.

Accumulation M selective energy spectra will provide an estimate of the SPD:

$$P_x(k) = \sum_{j=1}^{M} \left| X_j(k) \right|^2. \quad (2)$$

Fig. 1 shows the SPD graph of the acoustic signal of a screw-motor-driven unmanned aerial vehicle (UAV), obtained with the following periodogram parameters: $N_{FFT} = 8192$, $M = 3$, $R = 0{,}5\ N_{FFT}$ – and a rectangular window. The sampling frequency is $F_s = 44{,}1$ kHz, which is the standard value for most audio recording devices. The harmonic components of the spectrum, modulated by the noise component, follow frequencies that are multiples of the engine speed. The amplitude of the harmonics decreases with increasing frequency, but we can observe that some harmonics with higher frequencies exceed the previous ones, and some are not distinguishable at all against the background noise.

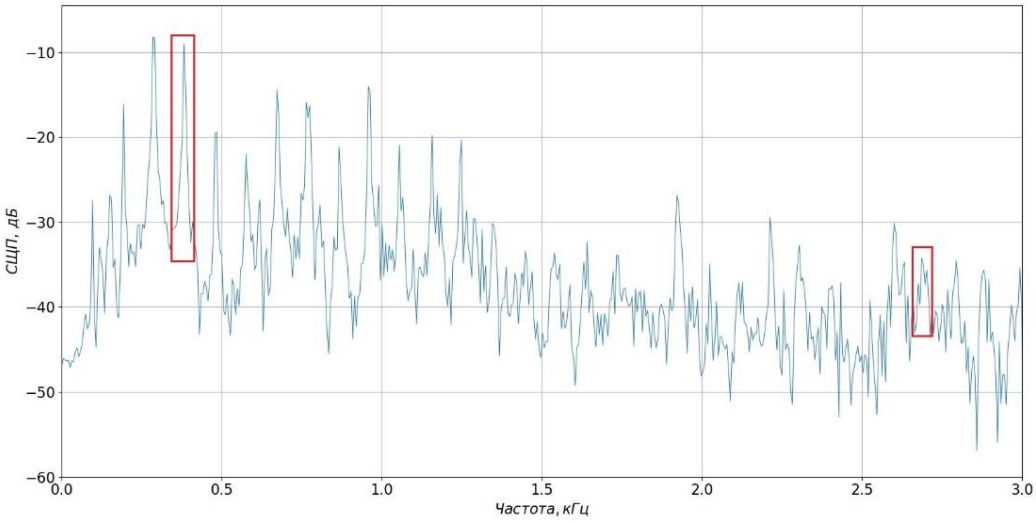

Fig. 1. SPD graph of theacoustic signal of a rotary-wing UAV

This occurs because acoustic waves are affected by many factors during their propagation (air temperature, precipitation, wind, humidity, etc.). In addition, the intensity of the acoustic field at the signal registration point changes during AAW maneuvering. Therefore, we can conclude that the amplitude of harmonic components is random and is an uninformative parameter.

The average noise level is unevenly distributed, with fluctuations ranging from 5 to 10 dB. As the frequency increases, there is a decrease in the power of both harmonic and noise components. This is due to atmospheric attenuation. The attenuation coefficient largely depends on the frequency of the sound; up to 1 kHz, its effect is insignificant. In addition, it is influenced by air temperature and humidity.

The harmonic of an acoustic signal is not a perfect pure tone oscillation, but occupies a certain width. Figure 2 shows an enlarged image of the harmonics of the acoustic signal of a screw motor ZPN at frequencies of about 380 Hz and 2680 Hz, highlighted by rectangles in Figure 1. The peak width at the noise level is about 40 Hz. Its shape with a higher frequency is more extended, which is caused by the Doppler effect.

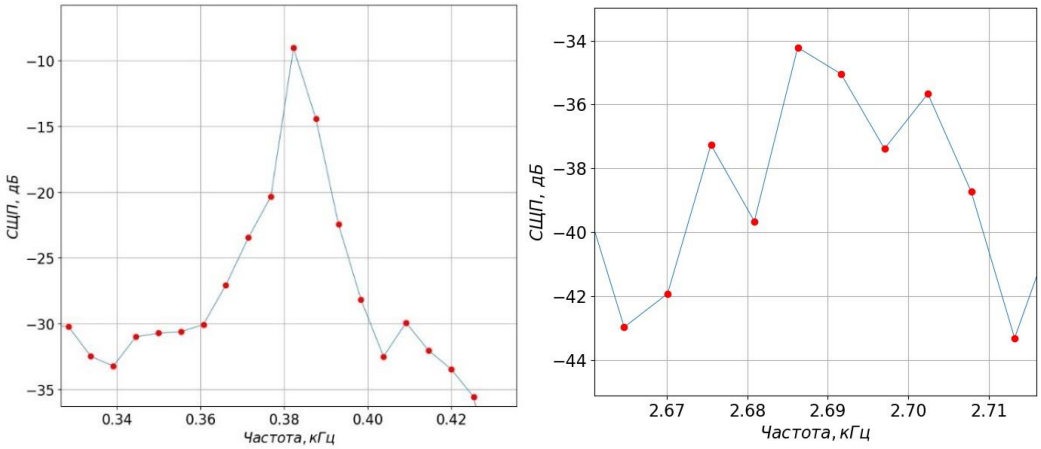

Fig. 2. Harmonics of the acoustic signal of a screw-motor UAV

For the above sampling frequency and periodogram window size, this peak width is $K_p = 8$ requency spectrum counts, and their period is – K_c = 18–19 counts.

In the group signal of the UAV shown in Fig. 3, extended harmonics are observed due to the multiplication of peaks shown in Fig. 4. This occurs because acoustic emissions from several UAVs simultaneously arrive at the microphone, but the frequencies of the harmonic components do not coincide, as they depend on the position of the UAV relative to the microphone, its speed, and the engine operating mode. When the frequency mismatch is greater than the harmonic width of the individual AAW signal, they are observed separately. The size of the extended harmonics varies and ranges from 18 to 25 frequency counts.

Therefore, the group acoustic signal of screw motor AAW is saturated with harmonic components and has significant noise level fluctuations, so the fixed threshold harmonic detection method is not effective. To detect a greater number of harmonic components, it is advisable to use adaptive threshold processing methods that are capable of tracking changes in noise level and harmonic components. Such methods include CFAR algorithms, which are widely used in the detection of radar signals [12].

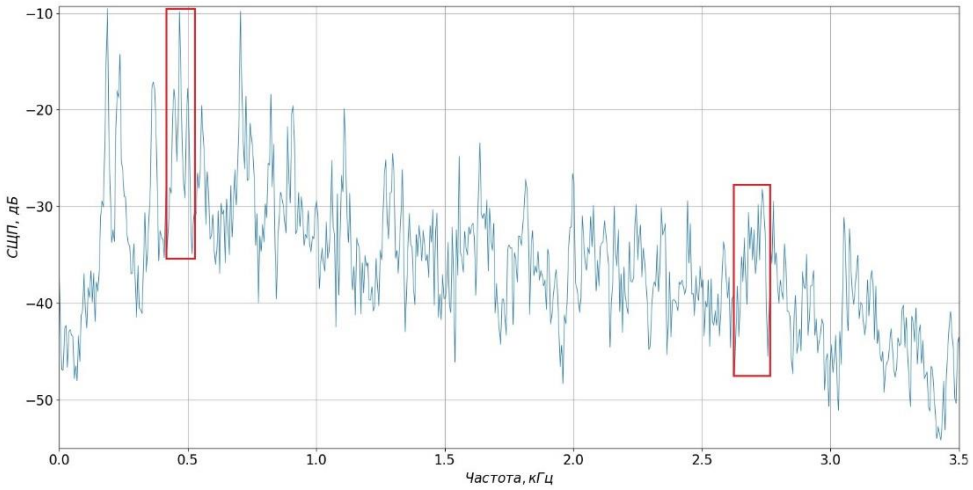

Fig. 3. SPD graph of the group acoustic signal of three UAVs

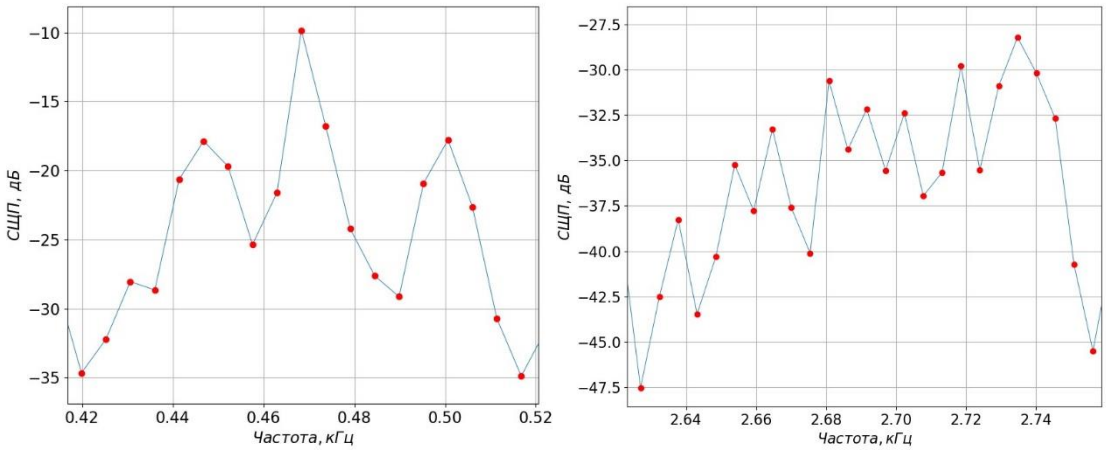

Fig. 4. Harmonics of the group acoustic signal of three UAVs

Analysis of known CFAR algorithms and features of their application

The CFAR algorithm is an adaptive threshold processing method that is widely used in radar to detect targets in conditions of uneven noise levels, interference, and signal interference. Thanks to the adaptability of the threshold level, it is capable of providing better detection quality than the fixed threshold method, whose effectiveness deteriorates when the signal-to-noise ratio changes [2].

In the CFAR algorithm, the average noise power is estimated using a sliding window centered on the test count (TC), which is checked for the presence of reflected signal energy. It includes guard intervals. K_s and assessment intervals K_e on both sides of the TC. The structure of the sliding window algorithm is shown in Fig. 5. The TC noise level is estimated based on the statistics of the front counts. K_{ef} and rear K_{er} assessment intervals. Countdown of protective intervals K_s are not used to assess noise levels, as they may contain values related to TC, which would lead to a bias in the noise level assessment.

The sliding window moves through the data array, shifting one count at a time. At each position, a detection decision is made—whether the TC exceeds the threshold level determined based on the noise in the interval. K_e. There are several approaches to assessing background noise levels, which are used in different wave propagation and signal conditions. Let's consider some of them.

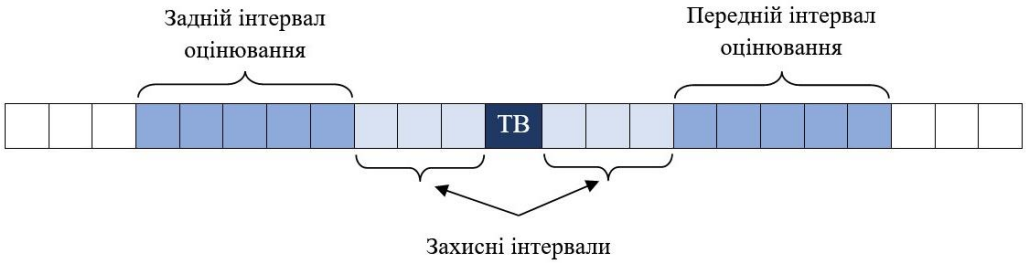

Fig. 5. Structure of a sliding window

Cell averaging (CA-CFAR) is one of the simplest processing methods. The TC noise level is calculated as the average value of counts in the interval K_e:

$$\sigma_i = \frac{1}{K_e}\sum_{k=1}^{K_e} P_x(k). \tag{3}$$

Based on this, the detection threshold is determined using the following expression:

$$T = \alpha \cdot \sigma, \tag{4}$$

where α – scaling factor, which is a function of the false alarm probability P_{FA} and the number of counts in the interval K_e.

The detection threshold varies depending on the noise level and has a higher value on both sides of the counts containing the energy of the reflected signal. This method is optimal for uniform background noise distribution. Its disadvantage is the masking of closely spaced signals in a multi-signal environment. The masking effect occurs when a closely spaced signal that is not related to the TC signal falls within the evaluation interval and shifts the threshold value.

CFAR algorithm, in which only counts from one of the evaluation intervals are used to calculate the threshold (K_{ef} or K_{er}), can detect two close signals. In this method, the noise level is determined separately for K_{ef} and K_{er}, then take the smaller of the two values (smallest of CA – SOCA-CFAR) and calculate the threshold level. If there are more than two close signals, this algorithm can only detect one of them.

A more sophisticated approach to noise assessment is a method in which interval counts K_e first sorted from smallest to largest value (order statistics CFAR – OS-CFAR). From the ordered sequence, take *k*-th highest count as noise level. This method is robust in a multi-signal environment, but has greater computational complexity.

Common disadvantages of CFAR algorithms include possible self-masking of wideband signals and signal-to-noise ratio loss. The self-masking effect occurs when the signal bandwidth is greater than the guard interval. Another defect is related to the fact that the CFAR threshold is on average higher than the threshold constructed according to the Neyman-Pearson criterion for known noise distribution parameters [12].

Choosing the type of algorithm and its parameters

The parameters that are set for a specific implementation of the CFAR algorithm are the values of the intervals K_s and K_e, as well as the false alarm probability value P_{FA}. The effectiveness

of the CFAR algorithm depends on its settings. In this study, we use the CFAR algorithm to detect harmonics in an acoustic signal, so we set the interval sizes based on their width and tracking period.

The study found that the protection interval must be at least greater than the width of the acoustic signal harmonic $K_s > K_p$, so that readings belonging to it are not used to determine the noise level. The evaluation intervals, in turn, should not exceed the distances between adjacent harmonics. $K_{ef} < K_c$, $K_{er} < K_c$. Failure to comply with these requirements will result in a shift in the noise level and detection threshold assessment. For the acoustic signal of a single UAV, we set the following parameter values: $K_s = 5$, $K_e = 18$ and $P_{FA} = 10^{-2}$.

The acoustic signal spectrum may contain intervals where harmonics are weakly distinguished against the background noise (for example, the frequency band from 1.2 kHz to 2.2 kHz (Fig. 1)) and, accordingly, they are more difficult to detect compared to more powerful ones. Fig. 6 shows the results of the CA-CFAR, SOCA-CFAR, and OS-CFAR algorithms in this interval. As can be seen, the threshold shape of each algorithm tracks the peaks of the acoustic signal harmonics. However, the CA-CFAR and SOCA-CFAR levels are slightly higher than OS-CFAR, which causes them to miss some peaks.

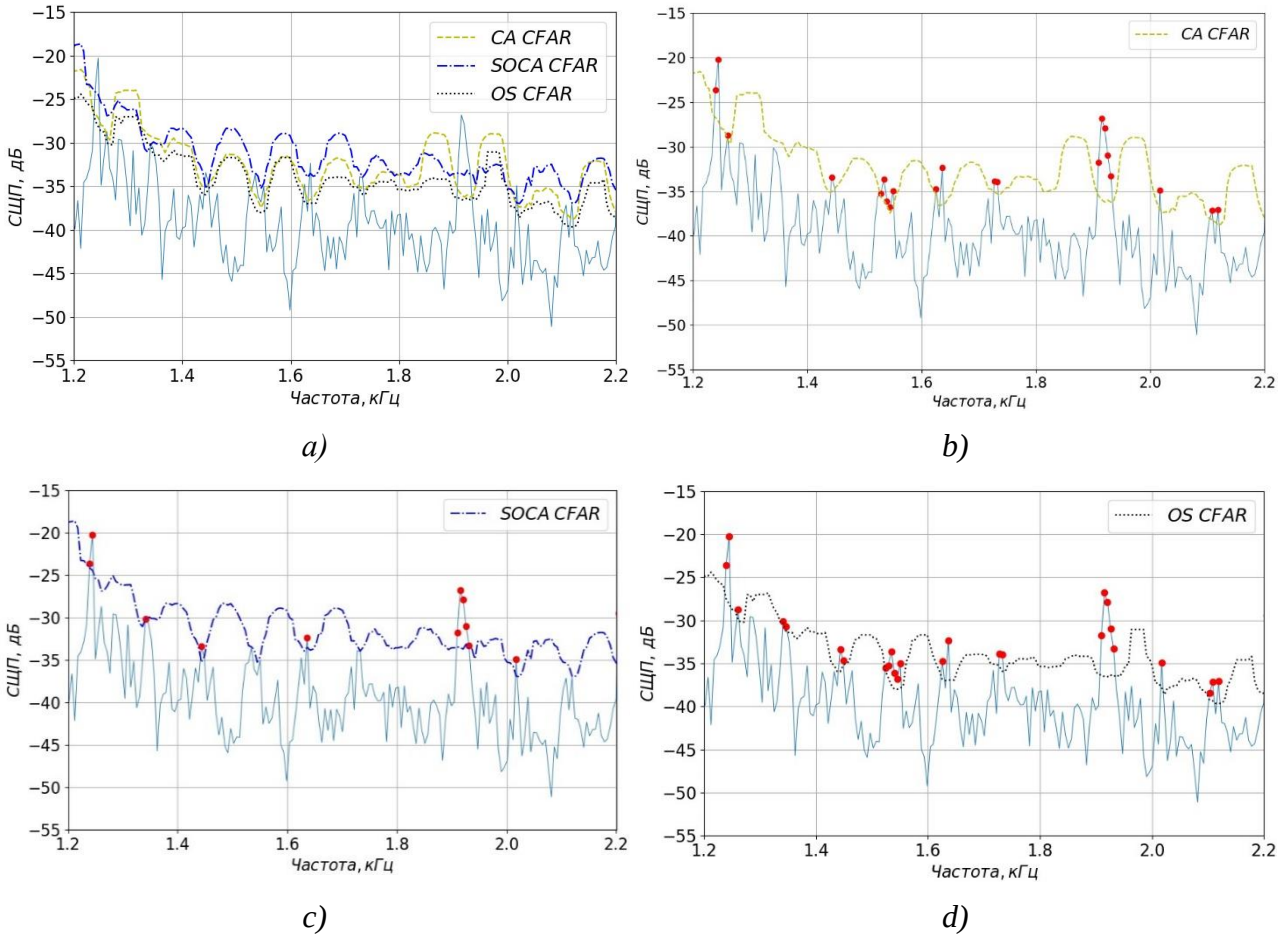

Fig. 6. Detection of harmonics in the acoustic signal of a single UAV: a) comparison of algorithms; b) CA-CFAR; c) SOCA-CFAR; d) OS-CFAR

The significance of false alarms in this study is not as critical as in radar operation, because the detected harmonic frequencies are subject to further logical processing, and false values will be filtered out, so it can be selected to ensure the detection of as many harmonic peaks as possible.

In the case of a group acoustic signal, the process of detecting harmonics becomes significantly more complicated. A set of peaks with different widths and follow-up periods requires a more flexible approach. Fig. 7a shows the operation of CFAR algorithms with the same settings as in the previous case. The effect of masking close peaks is evident, and the threshold shape does not correspond to the noise level fluctuation in the signal.

To detect more harmonics, it is necessary to increase the K_s interval to the width of the harmonic groups and determine the interval value K_e. As we can see, its insufficient width (Fig. 7b) leads to significant fluctuations in the threshold level, since only a small number of noise readings are used for calculations. In addition, in the interval K_e signal harmonics are picked up and shift the threshold. It should be noted that too high a value K_e increases computation time, which affects system performance in real time. Fig. 7c and Fig. 7d illustrate the operation of algorithms with values K_e = 20 and K_e = 30 counts respectively.

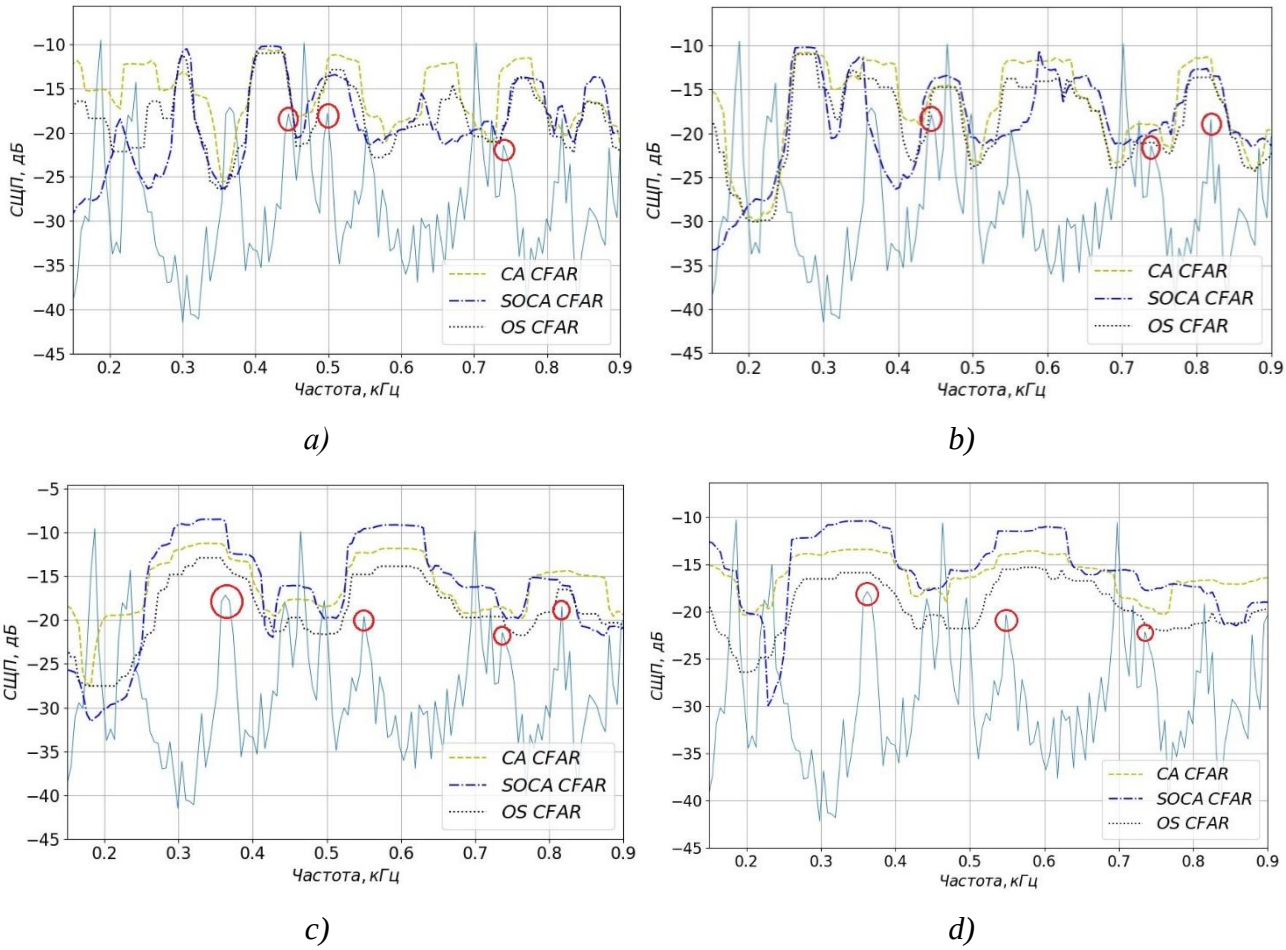

Fig. 7. Detection of harmonics of the group acoustic signal of the UAV at different intervals K_s and K_e: a) 5, 9; b) 12, 9; c) 12, 20; d) 12, 30

From the above, it follows that when K_e increases, the threshold of the OS-CFAR algorithm decreases significantly compared to CA-CFAR and SOCA-CFAR, and its shape becomes

smoother. This can be explained by a fundamental difference in the calculation of the threshold level. The algorithm under study allows discarding any number of readings containing harmonic component energy, as well as estimating the noise level using a wider range of values.

Figure 8 below shows the operation of the OS-CFAR algorithm with a group acoustic signal in the frequency band up to 3 kHz. As we can see, decreasing the number of the *k*-th count from the ordered statistics of the K_e interval values causes a decrease in the detection threshold, as well as reduces the steepness and amplitude of its fluctuations. This, in turn, allows for an increase in the number of detected harmonics, as demonstrated in Fig. 8b at frequencies from 2 kHz to 2.5 kHz.

Thus, based on the analysis, it can be concluded that the OS-CFAR algorithm allows detecting close peaks in the group acoustic signal of propeller-driven UAVs both in the low-frequency range, where harmonics significantly exceed the noise level, and in the higher-frequency range, where they are weakly distinguished against the noise background.

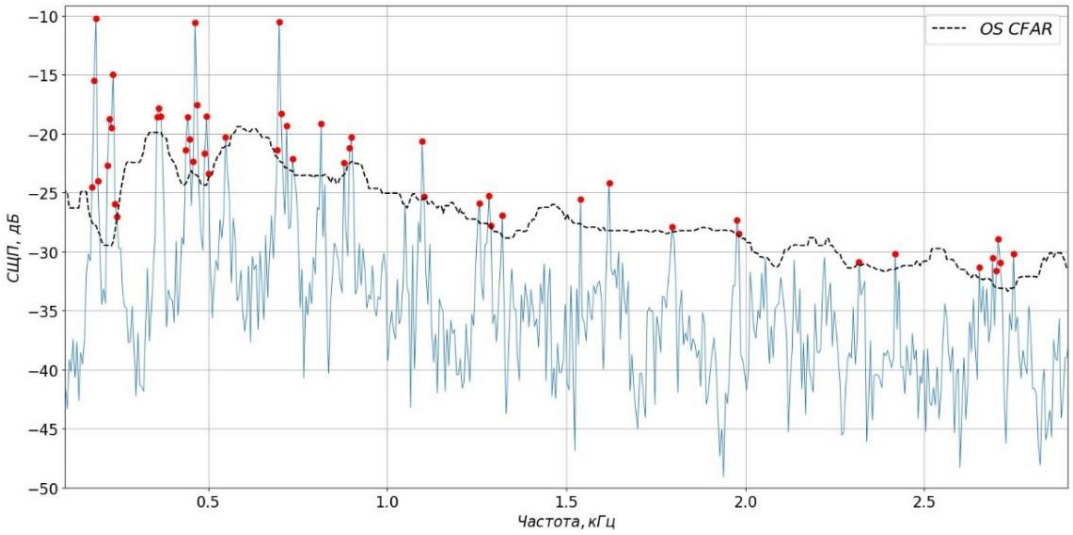

a)

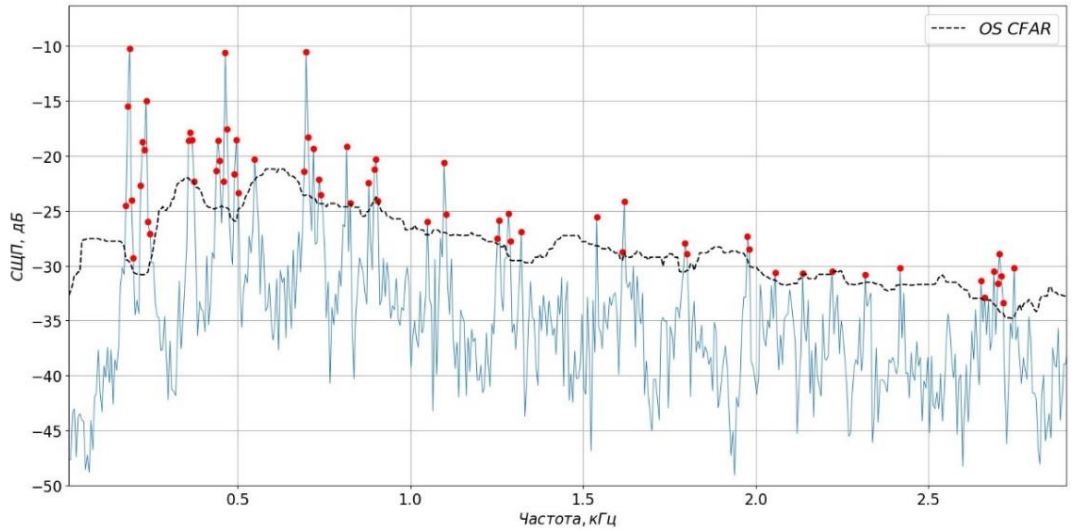

b)

Fig. 8. Detection of harmonics in the group acoustic signal of a UAV using the OS-CFAR algorithm: a) k = 0,6 K_e; b) k = 0,5 K_e

Research on the proposed approach

To determine the gain in the number of detected harmonics compared to similar detection methods that do not require preliminary noise estimation, an experiment was conducted, which showed that the OS-CFAR algorithm detects on average 45% more harmonics than the consecutive mean excision (CME) algorithm [13] algorithm and 26% more than the moving average (MA) algorithm. The testing was carried out using 100 implementations of a group acoustic signal of a UAV in the frequency band from 0 kHz to 3 kHz. An example is shown in Fig. 9.

We can conclude that the CME algorithm works in areas where the noise level is uniform, but does not track intervals when the power of noise and harmonic components decreases due to atmospheric attenuation.

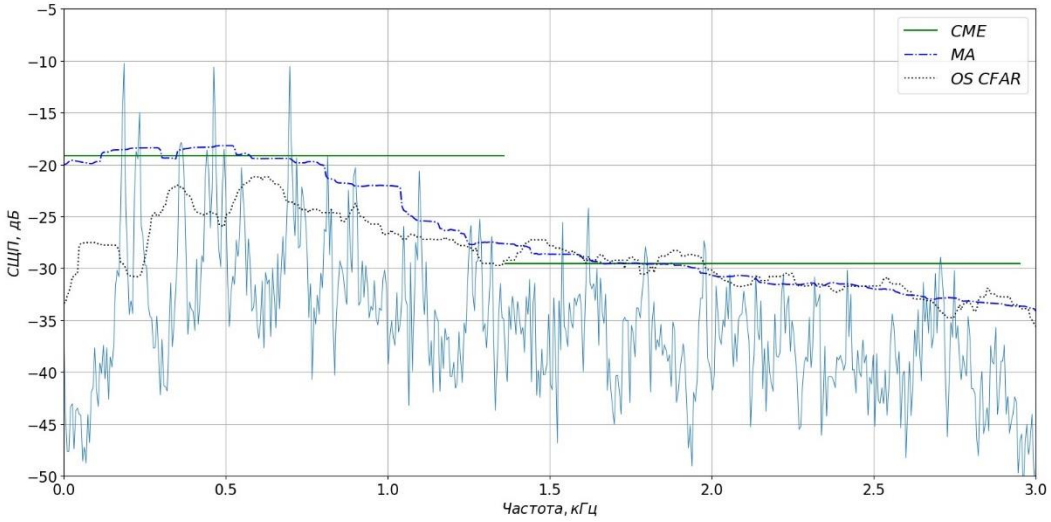

Fig. 9. Comparison of methods for detecting harmonic components of a signal

The MA algorithm works best in the frequency range above 1 kHz, where harmonics slightly exceed the noise level. In the frequency range up to 1 kHz, it misses less powerful peaks in group harmonics. This is a negative factor, because their presence indicates the number of separate acoustic signal sources.

Conclusion. The study found that the OS-CFAR algorithm is best for detecting the maximum number of harmonic components in the acoustic signal of a screw motor AAW. The experiment showed that with the appropriate algorithm settings (K_s = 12, K_e = 30 for F_s = 44,1 kHz) the proposed method may provide better results compared to other detection methods.

The results obtained can be used to improve existing devices and systems for acoustic monitoring of airspace and to develop new ones.

Prospects for further research in this area lie in the development of algorithms for logical processing of detected harmonic components to separate the number of AAW in a group acoustic signal.

REFERENCES

1. Pozdniakov, V. V., Buhaiov, M. V. (2023). Analiz akustychnykh syhnaliv zasobiv povitrianoho napadu [Acoustic Signals Analysis of Aerial Attack Weapon]. *Problemy stvorennia,*

vyprobuvannia, zastosuvannia ta ekspluatatsii skladnykh informatsiinykh system: zb. nauk. prats. [Problems of Construction, Testing, Application and Operation of Complex Information Systems. Scientific Journal of Korolov Zhytomyr Military Institute], *25* (I), 58–75. https://doi.org/10.46972/2076-1546.2023.25.06 [in Ukrainian].

2. Mark, A. (2014). Richards. Fundamentals of Radar Signal Processing. 2 nd Ed. ISBN: 978-0-07-179832-7.

3. Kang, M., Leng, X., & Lin, Z. et al. (2017). A Modified Faster R-CNN Based on CFAR Algorithm for SAR Ship Detection. In *International Workshop on Remote Sensing with Intelligent Processing (RSIP).* Shanghai, China. (pp. 1–4). https://doi.org/10.1109/RSIP.2017.7958815

4. Xiao Jialin, LI Yu, & Yuan Qinglong et al. (2022). Dropout Regularization Method of Convolutional Neural Network Based on Constant False Alarm Rate. *Journal of East China University of Science and Technology, 48* (1), 87–98. https://doi.org/10.14135/j.cnki.1006-3080.20201127005

5. Jue Gao, Haisen Li, Baowei Chen et al. (2017). Fast Two-Dimensional Subset Censored CFAR Method for Multiple Objects Detection from Acoustic Image. *IET Radar, Sonar & Navigation, 11,* 3, 505–512. https://doi.org/10.1049/iet-rsn.2016.0322

6. He Di, Leung Henry. (2008). Network Intrusion Detection Using CFAR Abrupt-Change Detectors. *IEEE Transactions on Instrumentation and Measurement, 57,* 3, 490–497. https://doi.org/10.1109/TIM.2007.910108

7. He Di, Leung Henry. (2009). Network Intrusion Detection Using a Stochastic Resonance CFAR Technique. *Circuits Syst Signal Process, 28,* 361–375. https://doi.org/10.1007/s00034-008-9087-y

8. AsSadhan, B., AlShaalan, R., & Diab, D. M. et al. (2020). A Robust Anomaly Detection Method Using a Constant False Alarm Rate Approach. *Multimed Tools Appl, 79,* 12727–12750. https://doi.org/10.1007/s11042-020-08653-8

9. Wang, B., Li, S., & Li, A. et al. (2024). Location Method for Cable Defects Based on Frequency Domain Reflectometry-Constant False Alarm Rate. In *20th International Conference on AC and DC Power Transmission (ACDC–2024).* Shanghai, China. (pp. 183–189). https://doi.org/10.1049/icp.2024.2274

10. An, G., Huang, Z., & Li, Y. (2023). Constant False Alarm Rate Detection of Pipeline Leakage Based on Acoustic Sensors. *Sci Rep., 13,* 14149. https://doi.org/10.1038/s41598-023-41177-3

11. Kundu, D., & Nandi, S. (2012). *Statistical Signal Processing: Frequency Estimation.* Springer, New Delhi, Heidelberg, New York, Dordrecht, London.

12. Mark A. Richards, James A. Scheer, William A. Holm. (2010). *Principles of Modern Radar. Vol. I: Basic Principles.* ISBN: 978-1-891121-52-4. https://doi.org/10.1049/sbra021e

13. Vartiainen, J., Lehtomäki, J., & Saarnisaari, H. et al. (2010). Analysis of the Consecutive Mean Excision Algorithms. *Journal of Electrical and Computer Engineering,* 459623. https://doi.org/10.1155/2010/459623